Research Square

Preprints are preliminary reports that have not undergone peer review. They should not be considered conclusive, used to inform clinical practice, or referenced by the media as validated information.

Metatranscriptomic analyses reveal ruminal pH regulates fiber degradation and fermentation by shifting the microbial community and gene expression of carbohydrate-active enzymes

MengMeng Li (mengli@vt.edu)
Virginia Polytechnic Institute and State University https://orcid.org/0000-0001-5958-0941

Robin R. White
Virginia Polytechnic Institute and State University

Le Luo Guan
University of Alberta

Laura Harthan
Virginia Polytechnic Institute and State University

Mark D. Hanigan
Virginia Polytechnic Institute and State University

Research Article

Keywords: Metatranscriptomics, Microbiome, pH, Rumen

Posted Date: November 13th, 2020

DOI: https://doi.org/10.21203/rs.3.rs-32565/v2

License: This work is licensed under a Creative Commons Attribution 4.0 International License. Read Full License

Version of Record: A version of this preprint was published at Animal Microbiome on April 23rd, 2021. See the published version at https://doi.org/10.1186/s42523-021-00092-6.

Abstract

Background: Volatile fatty acids (VFA) generated from ruminal fermentation by microorganisms provide up to 75% of total metabolizable energy in ruminants. Ruminal pH is an important factor affecting the profile and production of VFA by shifting the microbial community. However, how ruminal pH affects the microbial community and its relationship with expression of genes encoding carbohydrate-active enzyme (CAZyme) for fiber degradation and fermentation are not well investigated. To fill in this knowledge gap, six cannulated Holstein heifers were subjected to a continuous 10-day intraruminal infusion of distilled water or a dilute blend of hydrochloric and phosphoric acids to achieve a pH reduction of 0.5 units in a cross-over design. RNA-seq based transcriptome profiling was performed using total RNA extracted from ruminal liquid and solid fractions collected on day 9 of each period, respectively.

Results: Metatranscriptomic analyses identified 19 bacterial phyla with 156 genera, 3 archaeal genera, 11 protozoal genera, and 97 CAZyme transcripts in sampled ruminal contents. Within these, 4 bacteria phyla (*Proteobacteria*, *Firmicutes*, *Bacteroidetes*, and *Spirochaetes*), 2 archaeal genera (*Candidatus Methanomethylophilus* and *Methanobrevibacter*), and 5 protozoal genera (*Entodinium*, *Polyplastron*, *Isotricha*, *Eudiplodinium*, and *Eremoplastron*) were considered as the core active microbes, and genes encoding for cellulase, endo-1,4-beta- xylanase, amylase, and alpha-N-arabinofuranosidase were the most abundant CAZyme transcripts distributed in the rumen. Rumen microbiota is not equally distributed throughout the liquid and solid phases of rumen contents, and ruminal pH significantly affect microbial ecosystem, especially for the liquid fraction. In total, 21 bacterial genera, 4 protozoal genera, and 6 genes encoding CAZyme were regulated by ruminal pH. Metabolic pathways participated in glycolysis, pyruvate fermentation to acetate, lactate, and propanoate were downregulated by low pH in the liquid fraction.

Conclusions: The ruminal microbiome changed the expression of transcripts for biochemical pathways of fiber degradation and VFA production in response to reduced pH, and at least a portion of the shifts in transcripts was associated with altered microbial community structure.

Introduction

In the modern cattle industry, high-concentrate diets (50 to 90% grain) are often fed to maintain high milk or meat production. High-concentrate diets can stimulate rumen fermentation by resident microorganisms, producing more volatile fatty acids (VFA) including acetate, propionate, and butyrate and sometimes lactic acid [1, 2]. When VFA or lactic acid accumulate in the rumen, ruminal pH will rapidly drop which is associated with altered microbial ecology and metabolic disorders such as clinical or subclinical rumen acidosis [3-6]. Studies have indicated that the activity or numbers of cellulolytic microbes are inhibited if ruminal pH is less than 6.0, primarily due to the regulation of intracellular pH, resulting in inhibition of cellobiose transport activity [7, 8]. Consequently, fiber degradation and VFA production decrease when pH drops below critical values [9].

Intraruminal VFA production is of paramount importance as it provides up to 75% of total metabolizable energy in ruminants [1, 2], and individual VFA have distinct metabolic fates [9]. The production of VFA shares glycolysis as a common pathway with pyruvate as the central branching point, and conversion of pyruvate to individual VFA is driven by carbohydrate-active enzyme (CAZyme) produced by microorganisms in the rumen [10]. Various *in vitro* studies indicated pH significantly affects the profile and production of VFA [11-13]. Changes in VFA profile and production appear to occur through a shift in the biochemical pathways expressed by the overall microbial population in the rumen. However, the gene expressions of CAZyme in response to pH reductions and associations between rumen microbiota and CAZyme gene expressions have not been well investigated.

High-throughput sequencing techniques such as metatranscriptomics can analyze transcripts expressed by a microbial community at a specific point in time, which allows a simultaneous investigation of gene expressions and abundance of active microbiomes in an ecosystem [14]. In this work, we used metatranscriptomic analyses to investigate how reduced ruminal pH altered the microbial community, expression of CAZyme transcripts, fiber degradation and VFA concentrations following a continuous 10-day intraruminal acid infusion. We hypothesized that low pH would alter biochemical pathways to affect fiber degradation and VFA production via a shift in microbial community structure and their expressions of CAZyme genes in the rumen.

Methods

Animals, experimental design, and feeding management

Six cannulated Holstein heifers with an initial BW of 362 ± 22 kg (mean ± SD) were subjected to each of 2 treatments in a two-period, cross-over design. The treatments were 10 days of continuous intraruminal infusions of distilled water (Control) or a dilute blend of hydrochloric and phosphoric acids to achieve 0.5 unit reduction in pH (LpH). There was a 5-day recovery period between the infusion periods.

The animals were housed in individual tie stalls during the infusions. They had continuous access to water, and were fed a common total mixed ration (TMR) formulated according to National Research Council recommendations [15]. Ingredient composition and nutrient content of the diet are listed in Table S1. The ration was fed every 4 hours with approximately 17% of the total daily feed allocated at each feeding to maintain stable rumen fermentation rates. Feed offered and refused was recorded at each feeding time and used to calculate daily feed intake.

The acid solution consisted of 73 g H_3PO_4, 185 g HCl and 800 g distilled water. Infusates were delivered into the rumen using an indwelling infusion apparatus and clinical infusion pumps (LifeCare 5000, Abbott Laboratories, North Chicago, IL). Ruminal pH was monitored every 4 hours, and the acid infusion rate was varied by animal to achieve a ruminal pH between 6.0 and 6.1. When ruminal pH dropped below 6.0, the infusion rate was decreased by 10 ml/h, and the ruminal pH was rechecked in 30 to 60 minutes.

The infusion rate was adjusted upwards if ruminal pH was above 6.1. Water was infused at a constant rate of 25 ml/h in the Control animals.

Sample collection

Rumen sampling was conducted by placing 2 small tubes with an 8 mm diameter via the cannula into the rumen contents in different locations within the rumen (cranial and caudal areas of the rumen) to collect rumen fluid prior to each feeding. Multiple layers of nylon net were tied around the end of the tubes to filter out the solid fractions. A total of 10 ml of rumen fluid was drawn from the tubes at each sampling event. Ruminal pH was immediately measured using a portable pH meter (Starter 300, Ohaus, Parsippany, NJ), and ruminal liquid samples were stored at -20 °C until future VFA analyses.

Prior to the morning feeding on day 9 of each period, rumen contents including both liquid and solids were collected via the ruminal cannula for RNA extraction. Ruminal liquid samples were drawn from the tubes. Rumen solid samples were collected from multiple rumen locations (dorsal, ventral, cranial, and caudal areas of the rumen) and excess liquid removed by squeezing through four layers of cheesecloth. The collected liquid and solid samples were immediately flash-frozen in liquid nitrogen, crushed into small pellets, transferred to cryovials, and transported to the laboratory in liquid nitrogen. RNA extraction was completed within 12 hours to avoid RNA degradation.

The mixed ration was sampled daily and dried at 55°C in a forced-air oven for DM determination. Subsamples were ground to pass a 2-mm screen in a Wiley Mill (A.H. Thomas, Philadelphia, PA), and composited by period. A subsample of the 2 mm material was used for further *in-situ* tests, and additional subsample was ground through a 1mm screen (Cyclone lab sample mill, UDY Corporation, Fort Collins, CO) and used for chemical analyses.

In-situ degradability

In-situ degradation of dietary hemicellulose, cellulose, and lignin were determined by the nylon bag technique described by Ørskov and McDonald [16] on the last 3 days of each period. Briefly, approximately 5 g of dried, ground (2 mm) diet sample was weighed into duplicate 5 × 10 cm polyester bags (50 μm pore size, Ankom Technology, Macedon, NY) and suspended in the rumen in a large (36 × 42 cm) nylon mesh bag secured to the ruminal cannula via a nylon cord. The samples were inserted into the rumen of each heifer before the morning meal and removed after 2, 8, 12, 24, 36, and 48 hours of incubation. Degradation rates were estimated as described by Ørskov and McDonald [16] using a non-linear least squares regression procedure (NLI) in R (version 3.5.1) [17]. The equations fitted to the data were:

$$\text{Degraded}(t) = a + b\ (1 - e^{-K_d t}) \qquad (1)$$

$$\text{Effective degradability}(\%) = \text{a} + \frac{bK_d}{K_d + K_p} \qquad (2)$$

where *a* represented the soluble fraction (%), *b* represented the potentially degradable fraction (%), K_d represented the degradation rate constant for the b fraction (%/h), *t* represented incubation time in the rumen (h), and K_p was the outflow rate, which was assumed to be 4%/h according to Mertens [18].

Chemical analyses

Dry matter content was determined according to the National Forage Testing Association method 2.1.4 [19]. Neutral detergent fiber (NDF) was determined as described by Van Soest *et al.* [20] using heat-stable α-amylase (FAA, Ankom Technology, Macedon, NY) and sodium sulfite. Acid detergent fiber (ADF) and lignin concentrations were determined according to AOAC method 973.18 [21]. Ash content was determined according to AOAC method 942.05 [21]. Hemicellulose was calculated as the difference between NDF and ADF. Cellulose was calculated by subtracting ash and lignin from ADF.

For measurement of ruminal VFA concentrations, rumen fluid samples were thawed and composited by day, animal, and period. The samples were centrifuged for 30 min at 2,500 × *g* at room temperature to remove solid particles, and supernatant liquid was collected. An external tracer consisting of a mix of ^{13}C-labelled acetate, propionate, and butyrate was added to each liquid sample, then rumen liquid samples were derivatized, and the derivatives were analyzed for isotopic ratio using a Thermo Electron Polaris Q mass spectrometer in tandem with a Thermo Electron Focus gas chromatography (GC-MS; Thermo Electron Corporation, Austin, TX) as described by Kristensen [22].

RNA extraction and sequencing

RNA from ruminal liquid and solid samples was extracted using an RNA Clean & Concentrator kit from Zymo Research (Irvine, CA, USA), which included a bead-beating step to mechanically break microbial cell walls. DNA was removed by treatment with Baseline-ZERO™ DNase (Epicentre Biotechnologies, Madison, WI) following the manufacturer's instructions. The quality of total RNA was checked using a 2100 Bioanalyzer (Agilent Technologies, Palo Alto, California). Concentration of total RNA were determined using the Qubit® RNA Assay Kit (Thermo Fisher Scientific, Waltham, MA). DNA free, RNA samples were used for library preparation using the TruSeq™ RNA LT Sample Preparation Kit (Illumina). Following library preparation, the final concentration of cDNA in each library was measured using the Qubit® dsDNA HS Assay Kit (Thermo Fisher Scientific, Waltham, MA), and the average library size was determined using the Agilent 2100 Bioanalyzer (Agilent Technologies, Palo Alto, California). The libraries were then pooled in equimolar ratios of 2 nM, and 4 pM of the library pool was clustered using the Illumina's cBot (Illumina, San Diego, USA). The 150 bp, paired-end sequencing reaction was performed on a HiSeq 2500 platform (Illumina, San Diego, USA) at Molecular Research LP (MRDNA, Shallowater, Texas).

Transcriptome mapping

The quality of raw paired-end reads was evaluated using the FastQC program (http://www.bioinformatics.babraham.ac.uk/projects/fastqc/). Residual adaptor sequences, low quality

bases with quality scores below 20, and reads shorter than 50 bp were removed using the Trimmomatic program (version 0.36) [23]. The 16S and 18S rRNA reads were subsequently extracted from the filtered RNA dataset for taxonomic profiling using the SortMeRNA program (version 2.1) [24] through alignment with the rRNA reference databases SILVA_SSU, SILVA_LSU [25], and the non-coding RNA reference database Rfam 11.0 [26] following descriptions in Li *et al.* [27]. The remaining filtered reads were aligned to the UMD3.1 *Bos Taurus* reference genome [28, 29] with TopHat2 using the default setting to remove host reads (version 2.1.1) [30]. The filtered reads not matching the host genome were considered putative microbial mRNA and were selected for further functional analyses.

Taxonomic profiling of the rumen microbial community

The pipeline DADA2 (version 1.6) was used to infer amplicon sequence variants (ASVs) from the aligned total rRNA using R (version 3.4.3;) [17] as described by Callahan *et al.* [31]. Briefly, the following was completed in sequence. Forward and reverse reads were trimmed with a maximum number of expected errors of 2 based on their quality scores. Error rates were learned using 1 million training sequences each for forward and reverse reads, and the resulting specific error rates for each possible transition (such as A to C, A to G) were used to infer ASVs for each sample from the trimmed reads. The forward and reverse sequences were merged, chimeras were removed, and taxonomy was assigned by comparison to the SILVA database (version 138) [25] using the naïve Bayesian classifier algorithm [32]. The richness of taxa was presented as relative abundance using the phyloseq package (version 1.24.2) [33].

Identification of genes encoding CAZyme *and functional metabolic pathway analysis*

The putative microbial mRNA sequences were assembled using Velvet with a kmer size of 31 [34] and aligned with the CAZyme database [35] to annotate glycoside hydrolases (GH) [36-40], glycosyltransferases (GT) [41, 42], carbohydrate binding modules (CBM) [43], polysaccharide lyases (PL), and carbohydrate esterases (CE) [44]. Only the best alignments with expectation values lower than 1×10^{-4} were considered for functional gene annotation using the UBLAST algorithm implemented in USEARCH (version 9.2.64) [45]. To remove biases associated with the length of the transcript and the sequencing depth of a sample, transcripts per million (TPM) were used to normalize read count values. The metabolic pathway abundances of each sample were determined from the processed reads using the Human Microbiome Project Unified Metabolic Analysis Network (HUMAnN2) pipeline with default parameters [46]. HUMAnN2 utilized the UniRef and MetaCyc databases to characterize the microbial pathways present in samples, and relative abundances of functional pathways were used for further statistical analysis.

Statistical analysis

All statistical analyses were conducted using R software (version 3.5.1) [17]. Dry matter intake (DMI), ruminal pH, and VFA concentration data were summarized by day. Ruminal fiber (hemicellulose, cellulose, and lignin) degradability data were summarized by hour within a sampling period. Analysis of variance was conducted in a mixed model with treatment and period as fixed effects and animal as a random

effect. Day within animal was included as a repeated measure for DMI, ruminal pH, and VFA concentrations, and hour within animal was included as a repeated measure for ruminal fiber degradability. The interaction between treatment and day or hour was included as a fixed effect in the mixed model. Autoregressive covariance and heterogeneous variance were used in the repeated measures using the nlme package (version 3.1-137) [47]. The kinetic parameters associated with fiber degradation were analyzed using the lmer function in the lme4 package (version 1.1-17) [48].

In the current study, only microbial taxa with a relative abundance greater than 0.05% in at least 25% of populations were considered as being observed and used for the analysis. Because high-throughput sequencing generates compositional data (transcript proportions of total reads rather than absolute values) [49], they do not map to Euclidean space, which can be problematic for statistical analyses [49-52]. Therefore, compositional data need to be transformed before statistical analyses to avoid invalid conclusions [49, 53, 54]. The relative abundance and gene expression data were transformed to a centered log ratio:

$$[x_1 \quad x_2 \quad \dots \quad x_n] \Rightarrow \left[\log\left(\frac{x_1}{(x_1 \times x_2 \dots x_n)^{\frac{1}{n}}} + e - 1\right) \quad \log\left(\frac{x_2}{(x_1 \times x_2 \dots x_n)^{\frac{1}{n}}} + e - 1\right) \quad \dots \quad \log\left(\frac{x_n}{(x_1 \times x_2 \dots x_n)^{\frac{1}{n}}} + e - 1\right) \right] \quad (3)$$

where $(x_1 \times x_2 \dots x_n)^{1/n}$ represents the geometric mean of the vector. Zero value components should be excluded when dealing with log ratio transformation. However, the sequencing read counts contained an excessive number of zeros, which presents an obstacle for log ratio transformation [49], results in non-normality [53], can cause spurious correlations [54], and may contribute to high false positive issues [55]. This was resolved by replacement of zero count values prior to transformation based on posterior distribution using a Markov Chain Monte Carlo iterative algorithm in the zCompositions package (version 1.1.1) [56]. We added a constant of e-1 to all ratios prior to transformation to avoid negative values where e is Euler's number. With such an addition, if the gene or transcript counts equal the geometric mean, the log transformed value equals 1, so log transformed values above 1 indicate read counts greater than the geometric mean, and less than 1 indicate read counts lower than the geometric mean. Thus, the relationships among the features in the taxa and gene expression data were captured in the log ratio abundances, which have the mathematical property of real random variables and can be analyzed using standard statistical methods [49]. Ruminal pH effects within the liquid or solid fraction, and sample fraction effects across the entire pH range were analyzed using orthogonal contrasts in multiple comparisons. Significant differences were declared at $P < 0.05$.

Principal component analysis was performed using the factoextra package [57]. Pairwise correlations were conducted to explore associations among microbes and transcripts encoding CAZyme, ruminal pH, fiber degradation, and VFA concentrations using the Hmisc package [58]. Sample fractions were converted to binary variables with 1 representing liquid samples and 0 solid samples. To decrease the correlation matrix size, rows and columns were filtered if they did not contain at least one correlation coefficient with an absolute value greater than 0.5 and a P value less than 0.05. The correlation results

were visualized using corrplot package [59] in R, and network analysis was demonstrated using Cytoscape (version 3.7.1) software.

Results

Changes in ruminal community diversity

In total, 417.5 million sequences deriving from 24 samples with an average read length of 155 bp were obtained, with a mean of 17.4 million reads per sample. After removing low quality sequences, 93.7 % of reads remained for further processing. After aligning with the rRNA reference databases, 32.6% of sequences were classified as 16S and 18S rRNA, the rest were considered as putative mRNA.

Approximately 76 and 116 bacterial genera were identified in the ruminal liquid and solid fractions (Figure 1A and Table S2; $P < 0.001$). A lower pH environment tended to increase numbers of bacterial genera in the liquid fraction compared to normal pH (68 versus 83 bacteria genera; $P = 0.1$), while there was no difference in the solid fraction (116 versus 115 bacteria genera; $P = 0.87$). When considering the total number of individual bacterial taxa, Menhinick's index indicated low pH increased bacterial richness in the liquid fraction ($P = 0.02$) but did not affect the richness in the solid fraction ($P = 0.97$) compared to the corresponding Control group. Hill's ratio indicated the there was no pH effect in either fraction ($P > 0.05$). The Shannon-Wiener index indicated that low pH increased bacterial community diversity in the solid fraction compared to the liquid fraction at normal pH ($P < 0.001$), but it had no effect on the solid fraction ($P = 0.74$). Although the liquid fraction had a greater richness than the solid fraction ($P = 0.04$), the liquid fraction was less homogenous than the solid fraction ($P < 0.001$), which contributed to a lesser diversity in the liquid fraction than the solid fraction ($P < 0.001$).

About 10 and 9 protozoal genera were observed in the liquid and solid fractions (Figure 1B and Table S1). Ruminal pH did not significantly affect richness, evenness, or diversity. Greater evenness and diversity were observed in the solid fraction than the liquid fraction ($P = 0.004$ and 0.005) though the liquid and solid fractions had no difference in richness ($P = 0.31$).

Only 3 archaeal genera were identified in the rumen, and no significant difference was observed in terms of richness, evenness, and diversity between liquid and solid fractions in association with treatment.

Principle Component Analysis of Bacterial Phyla and Protozoal Genera

Principle component analysis was conducted to compare overall composition of bacterial phyla among all samples (Figure 2). The analyses indicated the first component accounted for 41.2 % of the total variation, and the second component accounted for 19.4% of the total variation (Figure 2A). The first component was negatively correlated with *Bacteroidetes* and *Kiritimatiellaeota*, and positively correlated with *Chloroflexi* and *Actinobacteria*; While the second component was negatively correlated with *Firmicutes* and *Proteobacteria*, and positively correlated with *Epsilonbacteraeota*, and *Synergistetes*. Although there was an overlap between the Control and LpH group, the second component can separate

different ruminal pH treatments (Figure 2B), and the first component can clearly separate ruminal liquid and solid fractions (Figure 2C).

Principle component analysis for protozoal genera are displayed in FigureS1. The first component accounted for 35 % of the total variation, and the second component accounted for 24.1% of the total variation. The first component was positively correlated with *Entodinium*, while negatively correlated with *Polyplastron* and *Eudiplodinium* (Figure S1A). There was a positive correlation between the second component and *Dasytricha* and a negative correlation with *Diplodinium*, *Blepharocorys*, and *Cycloposthium* (Figure S1A). Similar to the overall variance structure of bacterial phylum, the second component appeared to sperate different ruminal pH treatments (Figure S1B), and the first component separated different ruminal liquid and solid fractions (Figure S1C).

Changes of taxonomic distribution in the rumen

Overall, there were 19 active bacterial phyla with a relative abundance greater than 0.05% identified in all samples. The most abundant phyla were *Firmicutes*, *Proteobacteria*, *Bacteroidetes*, and *Spirochaetes* (Figure 3A). However, their proportions were dependent on treatments or rumen sample fractions. Approximately 25.5% *Firmicutes*, 34.5% *Proteobacteria*, 17.1% *Bacteroidetes*, and 9.3% *Spirochaetes* were distributed in the liquid fraction of the normal pH group, while there were 26.0% *Firmicutes*, 25.6% *Proteobacteria*, 16.0% *Bacteroidetes*, and 11.1% *Spirochaetes* in the liquid fraction of the LpH group. The population contained 33.2% *Firmicutes*, 27.6% *Proteobacteria*, 11.7% *Bacteroidetes*, and 14.1% *Spirochaetes* in the solid fraction of the Control groups, as compared to 18.2% *Firmicutes*, 32.6% *Proteobacteria*, 21.3% *Bacteroidetes*, and 6.4% *Spirochaetes* in the liquid fraction of the LpH group.

Analysis of variance results were presented in and Figure 3B and Table S3. The ruminal liquid fraction had greater proportions of *Bacteroidetes*, *Cyanobacteria*, *Kirtimatiellaeota*, *Lentisphaerae*, and *Verrucomicrobia* than that in ruminal solid fractions ($P < 0.05$), but lesser proportions of *Actinobacteria*, *Chloroflexi*, *Firmicutes*, *Patescibacteria*, and *Spirochaetes* ($P < 0.05$). Compared to normal pH, the low pH treatment increased the proportion of *Chloroflexi* in the liquid fraction ($P = 0.05$), and decreased the proportions of *Bacteroidetes*, *Patescibacteria*, and *Proteobacteria* ($P < 0.05$). However, no significant pH effect was observed in the solid fraction.

Analyses at the bacterial genus level were performed to gain further insights into changes in the taxonomic distributions. In total, 156 bacterial genera were identified in the samples, with 61 having relative abundances greater than 0.05% in all the samples. On average, *Succinivibrionaceae_UCG-002*, *Treponema_2*, *Fibrobacter*, *Ruminobacter*, *Christensenellaceae_R-7_group*, *Erysipelotrichaceae_UCG-004*, *Ruminococcus_2*, *Prevotella_1*, *Succinivibrionaceae_UCG-001*, and *CAG-352* were the 10 most abundant genera, accounting for 17.5, 8.9, 4.4, 4.1, 3.6, 3.0, 3.0, 2.9, 2.8, and 2.7% of total bacteria within liquid and solid samples (Figure 4A). In total, 43 bacterial genera had different proportions between the ruminal liquid and solid samples; 16 bacterial genera were affected by ruminal pH in the liquid fraction; only 5 bacterial genera were affected by pH in the solid fraction (Table S4).

Regardless of ruminal pH, the solid fraction had a greater proportion of *Atopobium*, *Olsenella*, *Prevotellaceae_NK3B31_group*, *Prevotellaceae_UCG-001*, *Prevotellaceae_UCG-004*, *Flexilinea*, *Acetitomaculum*, *Butyrivibrio_2*, *Christensenellaceae_R-7_group*, *Family_XIII_AD3011_group*, *Family_XIII_UCG-001*, *Lachnoclostridium_1*, *Lachnoclostridium_10*, *Lachnospiraceae_AC2044_group*, *Lachnospiraceae_NK3A20_group*, *Lachnospiraceae_NK4A136_group*, *Lachnospiraceae_XPB1014_group*, *Mogibacterium*, *Moryella*, *Pseudobutyrivibrio*, *Ruminococcus_9*, *Ruminococcaceae_UCG-004*, *Ruminococcaceae_UCG-014*, *Ruminococcus_1*, *Ruminococcus_2*, *Saccharofermentans*, *Selenomonas_1*, *Desulfovibrio*, *Treponema_2*, and *Pyramidobacter* than the liquid fraction ($P < 0.05$), and a lesser proportion of *Prevotella_1*, *Prevotellaceae_YAB2003_group*, *Elusimicrobium*, *Anaerovibrio*, *Asteroleplasma*, *Erysipelotrichaceae_UCG-004*, *Bibersteinia*, *Ruminobacter*, *Succinivibrio*, *Sphaerochaeta*, *Synergistes*, *Mycoplasma*, and *Cerasicoccus* ($P < 0.05$).

As displayed in Figure 4B and Table S4, compared to normal ruminal pH, low ruminal pH decreased *Prevotella*, *Prevotella_9*, *Anaerosporobacter*, *Lachnospiraceae_UCG-007*, *Pseudomonas*, *Succinimonas*, and *Succinivibrionaceae_UCG-002* in the liquid fraction ($P < 0.05$), and increased *Flexilinea*, *Mogibacterium*, *Papillibacter*, *Ruminococcaceae_UCG-010*, *Victivallis*, *Sediminispirochaeta*, *Treponema*, *Pyramidobacter*, and *Synergistes* in the liquid fraction ($P < 0.05$). Finally, low ruminal pH increased *Bifidobacterium* in the solid fraction ($P < 0.05$), and decreased *Lachnoclostridium_1*, *Ruminiclostridium_9*, *Desulfuromonas*, and *M2PT2-76_termite_group* ($P < 0.05$).

In total, 11 protozoal genera were identified through analysis of microbial composition, and 7 of them were observed in all the samples with relative abundances greater than 0.05% of the total population. As displayed in Figure S2, *Entodinium*, *Polyplastron*, *Isotricha*, *Eudiplodinium*, and *Eremoplastron* were highly abundant representing 67.9, 11.0, 9.6, 2.7, and 2.9% of the population in all the liquid and solid samples. The ruminal liquid fraction had lesser proportions of *Diploplastron* and *Eudiplodinium* than the solid fraction ($P < 0.05$; Table S5). Low pH decreased the proportion of *Entodinium* and *Isotricha* in the liquid samples ($P < 0.05$; Table S5). However, no significant pH effect was observed in the solid samples.

Candidatus Methanomethylophilus and *Methanobrevibacter* were the most abundant archaeal genera, accounting for approximately 54.3 and 25.1% of total ruminal archaea. Low ruminal pH did not change archaeal composition in either fraction. However, the ruminal solid fraction had a greater proportion of *Methanobrevibacter* than the liquid fraction ($P < 0.05$), and a lesser proportion of *Candidatus Methanomethylophilus* ($P < 0.05$; Table S6).

Changes in CAZyme transcripts expressed by rumen microbiota

In total, 97 transcripts encoding CAZyme were identified, and 88 had a relative abundance above 0.05% in all the samples. As displayed in Figure 5A, genes encoding cellulase, endo-1,4-beta- xylanase, amylase, and alpha-N-arabinofuranosidase were the most abundant transcripts in the liquid and solid fractions, accounting for 12.83, 11.87, 7.72, and 2.75 % of the total enzyme transcripts. As shown in Table S7 and Figure 5B, 8 transcripts were significantly affected by ruminal pH in the liquid fraction; 2 transcripts were influenced by ruminal pH in the solid fraction, and 16 transcripts had different distributions between the

liquid and solid fractions. Within them 2 transcripts were affected by both pH effect in the liquid fraction and sample fraction effect, and 1 was affected by ruminal pH effect in both liquid and solid fractions.

The expression of genes encoding glucan phosphorylase, glucosidase Cel1C, pectate lyase, rhamnogalacturonan acetylesterase, and UDP-3-0-acyl N-acetylglucosamine deacetylase were upregulated by lower ruminal pH in the liquid fraction ($P < 0.05$), while transcripts of glycosyl hydrolase family 16, putative glycosyl transferase, and sucrose alpha-glucosidase were downregulated ($P < 0.05$). Compared to the normal pH, the low pH environment decreased expression of genes encoding glycosyl hydrolase family 43 in the solid fraction ($P < 0.05$), while increased gene expressions of pectate lyase ($P < 0.05$). The ruminal liquid fraction contained a greater proportion of transcripts of alpha-glucosidase, amylase, beta-galactosidase, cellulase celA, glycosyl hydrolase family 57, penicillin-binding protein 1A, putative 4-alpha-glucanotransferase, putative alpha-xylosidase, putative carbohydrate-active enzyme, and sucrose alpha-glucosidase than the solid fraction ($P < 0.05$), while lesser transcripts of glucan 1,4-alpha-maltotetraohydrolase, glucan phosphorylase, glycoside hydrolase family 43, glycosyl hydrolase family 51, glycosyltransferase 36, and isoamylase domain/esterase family protein ($P < 0.05$).

Functional metabolic pathway analysis

In total, 51 metabolic pathways were identified through the HUMAnN2 pathway analysis, and 5 pathways were significantly different among treatments (Table 1). Low pH significantly decreased relative abundances of metabolic pathway participated in glycolysis I (from glucose 6-phosphate), glycolysis II (from fructose 6-phosphate), pyruvate fermentation to acetate and lactate, and pyruvate fermentation to propanoate in the liquid fraction ($P < 0.05$). However, no significant difference was observed in the solid fraction. The relative abundances of metabolic pathway related to glycolysis I (from glucose 6-phosphate), L-isoleucine biosynthesis I (from threonine), and pyruvate fermentation to acetate and lactate were greater in the solid fraction than in the liquid fraction ($P < 0.05$).

Intake, fiber degradation, and VFA concentrations

Real time pH over the whole experimental period were displayed in Figure S3. As designed, the mean ruminal pH achieved for the Control and LpH treatments were 6.44 and 6.09, respectively. Compared to the Control, DMI was inhibited by decreasing ruminal pH ($P = 0.04$, Figure 5A and Table S8).

In situ degradation of dietary DM, hemicellulose, cellulose, and lignin with respect to the rumen incubation time were displayed in Figure S4. Although the individual parameters a, b, and k_d were not affected by lower ruminal pH (Figure 5B and Table S8), effective degradabilities of dietary DM, hemicellulose, cellulose, and lignin were decreased ($P < 0.05$, Figure 5C). Decreased DMI and ruminal fiber degradability were associated with decrease of VFA concentrations and presumably production rates. As a result, concentrations of ruminal total VFA, acetate, propionate, butyrate, isobutyrate, valerate, and isovalerate were decreased in response to lower ruminal pH ($P < 0.05$; Figure 5A and Table S8).

Correlations between ruminal microbes and gene expressions of CAZyme

Pairwise correlations between microbes and transcripts encoding CAZyme are displayed in Figure 7. There were 45 microbes (41 bacterial genera and 4 protozoal genera) and 27 CAZyme transcripts that had at least one correlation coefficient above 0.5 or less than -0.5 which was the criteria for inclusion in the matrix regardless of ruminal liquid or solid fractions. However, there was no significant correlations identified among archaeal genera and transcripts encoding CAZyme.

Discussion

The distribution of active microbes in the rumen

While metagenomics can reflect the comprehensive diversity of all the active and inactive microorganisms, metatranscriptomics is a more reliable tool to obtain insights into the most active microorganisms. In the present study, *Proteobacteria*, *Firmicutes*, *Bacteroidetes*, and *Spirochaetes* were the most predominant active bacterial phyla regardless of liquid and solid fractions in the rumen. These results were consistent with bacterial phylum profiles in beef cattle under metatranscriptomic analyses [60]. Although same phyla were identified as dominant bacteria in metagenomic studies, their community structure is quite different with approximately 50.5, 29.8, and 10.6% of *Firmicutes*, *Bacteroidetes*, and *Proteobacteria* [61-64], implying there was a difference of bacterial community structure at the genomic and transcriptomic levels. Kang *et al.* [65] indicated the abundance of *Proteobacteria* was greater when derived from rumen RNA than from DNA, and this difference was validated using denaturing gradient gel electrophoresis (DGGE) and qRT-PCR techniques. Those findings may help explain observations herein of *Proteobacteria* being the dominant active phyla in the rumen.

Besides differences at the genomic and transcriptional levels, bacterial community structure can be influenced by diets or animal breed. Henderson *et al.* [63] indicated that *Prevotella*, *Butyrivibrio*, and *Ruminococcus*, as well as unclassified *Lachnospiraceae*, *Ruminococcaceae*, *Bacteroidales*, and *Clostridiales* are considered as a core microbiome at the genus level across a wide geographical range. Li *et al.* [66] reported that *Prevotella* (11.94%), *Treponema* (11.25%), unnamed *Succinivibrionaceae* (8.98%), unclassified *Bacteroidales* (6.05%), and *Fibrobacter* (6.01%) were the most abundant active bacterial genera in the rumen. Although most of these genera were also identified as dominant taxa in the current study, their proportions were quite different, suggesting that the bacterial community structure could be caused by diet or breed effect, as high grain diet was fed to beef cattle in the previous study.

As expected, no unique taxonomic groups were identified for the solid and liquid environment, since they are prone to continuous interaction and mutual influences [64]. Substantial differences in terms of relative abundance of specific taxa were observed. The difference in microbial composition has previously been observed to be associated with substrate availability [67-69], rumen kinetics with respect to particle size [70], and physical and chemical properties [71]. We found that free-floating bacteria that readily degrade metabolizable carbohydrate, such as *Bacteroidetes* and *Lentisphaerae*, were more prevalent in the liquid fraction, while the cellulolytic bacteria, such as *Firmicutes* and *Spirochaetes*, are prominent members in the solid fraction. These results were consistent with previous studies [64, 69, 72].

Candidatus Methanomethylophilus and *Methanobrevibacter* were the most abundant archaeal genera based on transcript activity. Similar results were reported by Wang *et al.* [73] for black goats. A greater proportion of the archaeal genus *Methanobrevibacter* was observed in the ruminal solid fraction compared with the liquid fraction, while *Candidatus Methanomethylophilus* were more abundant in the liquid than the solid fraction. Similar results were also reported by Henderson *et al.* [74] and De Mulder *et al.* [64]. The location differences are related to their potential metabolic functions. Borrel *et al.* [75] published the genome sequence of *Candidatus Methanomethylophilus alvus* isolated from human gut and reported this isolate had genes for methylotrophic methanogenesis from methanol and methylamines. *Methanobrevibacter* is a methanogen related to the bioconversion of cellulose fiber to methane through a symbiotic relationship with a rumen anaerobic fungus [76].

In the current study, *Entodinium* was the predominate protozoa genus in the rumen, which was consistent with previous studies [6, 77, 78]. *Entodinium* has been characterized as a starch feeder. Maltase and amylase activity was prevalent in the cell free extracts made from the *Entodinium* suspensions [79]. However, the rest of the protozoal genera were highly varied. Henderson *et al.* [63] demonstrated the variability of protozoa between and within cohorts of co-located animals was much greater than bacteria and archaea. We found that ruminal liquid had a lesser proportion of *Diploplastron* and *Eudiplodinium* than the solid fraction. However, De Menezes *et al.* [80] observed that protozoan communities were very similar between ruminal liquid and solid fractions. The protozoal community was affected by rumen sample fractions which might be caused by the factors related to ruminal dynamics and protozoa growth. Inversely related to the rumen retention time, liquid associated protozoa have a greater ruminal outflow rate than solid associated protozoa, which might result in a greater proportion of protozoa in the solid fraction.

Microbial community changes in response to ruminal pH

A reduction in ruminal pH by 0.5 units decreased the proportions of *Bacteroidetes*, *Patescibacteria*, and *Proteobacteria* in the liquid fraction but did not affect their proportions in the solid fraction, suggesting that *Bacteroidetes*, *Patescibacteria*, and *Proteobacteria* were less sensitive to low ruminal pH in the solid fraction than the liquid fraction. Schulze *et al.* [81] demonstrated that VFA concentrations declined and pH increased as the sampling location moved from the medial to the ventral part of the rumen. This was ascribed to greater rates of microbial fermentation occurring in the medial part of the rumen, while VFA absorption by the rumen epithelium occurs in the ventral part of the rumen. This pH gradient may explain the relative lack of a response to pH in the solid fraction. Microbes in that fraction may be selected for tolerance to low pH.

Petri *et al.* [61] reported that the relative abundance of *Prevotella*, *Acetitomaculum*, *Pseudobutyrivibrio*, *Selenomonas*, *Succinivibrio*, *Treponema*, and *vadinHA42* genera in the rumen fluid increased following a high grain diet challenge. Plaizier *et al.* [82] found the abundance of *Succinivibrio*in the rumen fluid increased when animals were challenged with a high grain diet. Surprisingly, none of these genera were significantly affected in our study except for *Treponema*, implying different mechanisms of action

leading to bacterial community shifts in response to increased grain load versus increased H^+ concentrations. High grain intake provides nonstructural carbohydrate substrate that results in greater energy for maintenance and growth of microbes with reduced pH occurring as a consequence of that fermentative activity. Conversely, acid infusion reduced ruminal pH without a change in substrate supply. Increased H^+ concentrations have been found to increase the transmembrane pH gradient and electrical potential, which requires energy to maintain physiological gradient given increased passive transport driven by the electrical gradient [7, 12]. Therefore, the increased maintenance activity might have contributed to inhibited transport activity and reduced microbial growth [7].

Franzolin and Dehority [83] reported that feeding a high concentrate diet increased the proportions of the protozoal genera *Isotricha* and *Epidinium*. *Hook et al. [84] found that a* high concentrate diet increased the number of *Entodinium*, *Ophryoscolex*, *Isotricha*, and *Dasytricha. These responses imply that any inhibition in growth caused by reduced pH is overwhelmed by the response to increased substrate supply. This is consistent with our observations of* decreased proportions of *Isotricha* and *Entodinium* in the liquid fraction *with* low ruminal pH in the absence of increased substrate supply.

The distribution of CAZyme transcripts in the rumen and associations with rumen microbes

Genes encoding for cellulase, endo-1,4-beta- xylanase, amylase, and alpha-N-arabinofuranosidase were the dominate enzyme transcripts in the rumen, which was consistent with previous studies. Cellulase has been assigned to multiple carbohydrate binding module families (CBM), and glycoside hydrolase families (GH). Wang *et al.* [85] indicated GH5 and GH9 were the most frequent cellulases found in a metagenomic study. Similar results were also reported in metatranscriptomic studies [10, 86]. Cellulase, endo-1,4-beta-xylanase, and alpha-N-arabinofuranosidase are important enzymes for cellulose and hemicellulose degradation [39]. The main function of cellulase is to hydrolyze 1,4-beta-D-glycosidic linkages to release individual monosaccharides [87]. Endo-1,4-beta- xylanase catalyzes the hydrolysis of glycosidic linkages in the xylan backbone [88]. Alpha-N-arabinofuranosidase cleaves arabinose from the xylose backbone, thus contributing to the degradation of hemicellulose. Amylases are a group of enzymes that hydrolyze glycosidic bonds present in starch, which have been grouped into multiple CBM families and GH13, 14, 15, 31, and 57. Deusch *et al.* [69] observed that GH 57 was the most abundant family across all samples in the rumen. Comtet-Marre *et al.* [89] reported amylases represent 20% of total GH in the rumen of dairy cows.

Carbohydrate-active enzymes are generally secreted by ruminal microbes. Based on this, the distribution of CAZyme genes would be expected to be associated with the locations of the microbial community. Correlations between rumen microbes and enzyme transcripts indicated that the microbial community patterns were strongly associated with the gene expression patterns in the liquid and solid sampling locations. Thus, our hypothesis of colocalization of microbes possessing genes for specific enzymes and the expression of such enzyme transcripts was supported. This implies that knowledge of the community structure can be used to predict community function without needed to assess community activity directly.

Nutritional consequence of low pH regulation

Dietary carbohydrates including hemicellulose, cellulose, and starch, are the primary fermentation substrates in the rumen. They are degraded to hexoses and pentoses, and fermented to VFA via pyruvate [2]. Previous studies indicated VFA concentrations were reliable indexes for the relative production rates [90, 91], although the manipulation of pH independent of VFA production in the current study may have partially delinked production and concentrations due to potential stimulation of transport activity [92]. France and Dijkstra [2] demonstrated that fermentation patterns are determined by the composition of the microbial population which is driven by substrate composition. Regardless of whether fermentation shifts due to a change in microbial structure or due to a change in the expression patterns of a constant structure, characterization of the transcriptome should provide insight into the pathways being used and the microbes expressing those genes.

Low ruminal pH for prolonged periods in the current work negatively affected DMI, fiber degradation, and VFA concentrations, which agreed with previous studies [3, 9, 13, 84, 93]. Stewart [94] reported that reducing pH from 7.0 to 6.0 inhibited cellulolytic activity in the rumen. Hu *et al.* [95] found an inhibitory effect of low pH on cellulose degradation when pH was below 6.0. Sung *et al.* [93] showed that lowering incubation media pH to 5.7 decreased bacteria attached to substrate. In the current study, low ruminal pH reduced proportions of metabolic pathway participated in glycolysis, pyruvate fermentation to acetate, lactate, and propanoate in the liquid fraction. At least a portion of the shift in the metabolic pathways was associated with the altered microbial structure. Therefore, low pH could alter metabolic pathways to affect fiber degradation and VFA production via a shift in gene expressions expressed by the microbes in the rumen.

Conclusions

Ruminal pH associated with sampling location of the rumen contents significantly affected the microbial ecosystem. Sixteen bacterial genera and 2 protozoal genera were affected by low ruminal pH in the liquid fraction, However, only 5 bacterial genera and none of protozoal genera were affected by low pH in the solid fraction, implying that microbes exhibited different acid resistance in the liquid and solid fraction. Forty-three bacterial genera, 2 protozoal genera, and 2 archaeal genera exhibited different proportions between ruminal liquid and solid fractions, which suggest that microbiota are not equally distributed throughout the liquid and solid phases of rumen contents.

Low ruminal pH for prolonged periods downregulated CAZyme transcripts and metabolic pathways associated with glycolysis and pyruvate fermentation, leading to decreased fiber degradation and VFA production, suggesting that the ruminal microbiome changed the expression of transcripts in response to reduced pH, and at least a portion of the shifts in transcripts was associated with altered microbial structure.

Abbreviations

DMI: dry matter intake

VFA: volatile fatty acids

TMR: total mixed ration

CAZyme: carbohydrate-active enzyme

Declarations

Ethics approval and consent to participate

This study was conducted in accordance with the Federation of Animal Science Societies' Guide for the Care and Use of Agricultural Animal in Research and Teaching and approved by the Virginia Tech Institutional Animal Care and Use Committee (IACUC#16-133).

Consent for publication

Not applicable.

Availability of data and material

All raw sequence data have been deposited in the NCBI Sequence Read Archive under accession number PRJNA497850.

Competing interests

The authors declare that they have no conflict of interest.

Funding

This work was supported by the Virginia Agricultural Council; the USDA National Institute of Food and Agriculture, Hatch project NC-2040; the College of Agriculture and Life Sciences Pratt Endowment at Virginia Tech; and the Alberta Livestock and Meat Agency Ltd. (Edmonton, Alberta, Canada) under grant number 2015F055R.

Authors' contributions

MHD and LH designed this study. MML and RRW conducted the animal trail and *in-situ* tests. MML collected and analyzed all the samples. MML, RRW and LLG conducted bioinformatics analysis. MML and MDH conducted statistical analyses. MML, RRW, LLG, and MDH were responsible for the data interpretation and manuscript writing. All authors read and approved the final manuscript.

Acknowledgements

We appreciate all efforts made by all staff members in the Kentland Farm Dairy Science Center of Virginia Tech. We thank all members from Dr. M. D Hanigan's group for their help on sampling.

References

1. Siciliano-Jones J, Murphy M. Production of Volatile Fatty Acids in the Rumen and Cecum-Colon of Steers as Affected by Forage: Concentrate and Forage Physical Form1. Journal of dairy science 1989, 72:485-492.
2. France J, Dijkstra J. Volatile fatty acid production. Quantitative aspects of ruminant digestion and metabolism 2005, 2:157-175.
3. Russell JB, Rychlik JL. Factors that alter rumen microbial ecology. Science 2001, 292:1119-1122.
4. McCann JC, Luan S, Cardoso FC, Derakhshani H, Khafipour E, Loor JJ. Induction of subacute ruminal acidosis affects the ruminal microbiome and epithelium. Frontiers in microbiology 2016, 7:701.
5. Wetzels SU, Mann E, Metzler-Zebeli BU, Pourazad P, Qumar M, Klevenhusen F, Pinior B, Wagner M, Zebeli Q, Schmitz-Esser S. Epimural indicator phylotypes of transiently-induced subacute ruminal acidosis in dairy cattle. Frontiers in microbiology 2016, 7:274.
6. Zhang J, Shi H, Wang Y, Li S, Cao Z, Ji S, He Y, Zhang H. Effect of dietary forage to concentrate ratios on dynamic profile changes and interactions of ruminal microbiota and metabolites in Holstein heifers. Frontiers in microbiology 2017, 8:2206.
7. Russell JB, Wilson DB. Why are ruminal cellulolytic bacteria unable to digest cellulose at low pH? Journal of dairy science 1996, 79:1503-1509.
8. Russell JB. Effect of extracellular pH on growth and proton motive force of Bacteroides succinogenes, a cellulolytic ruminal bacterium. Applied and environmental microbiology 1987, 53:2379-2383.
9. Dijkstra J, Ellis J, Kebreab E, Strathe A, López S, France J, Bannink A. Ruminal pH regulation and nutritional consequences of low pH. Animal Feed Science and Technology 2012, 172:22-33.
10. Dai X, Tian Y, Li J, Su X, Wang X, Zhao S, Liu L, Luo Y, Liu D, Zheng H. Metatranscriptomic analyses of plant cell wall polysaccharide degradation by microorganisms in the cow rumen. Appl Environ Microbiol 2015, 81:1375-1386.
11. Marounek M, Bartos S, Brezina P. Factors influencing the production of volatile fatty acids from hemicellulose, pectin and starch by mixed culture of rumen microorganisms. Zeitschrift für Tierphysiologie Tierernährung und Futtermittelkunde 1985, 53:50-58.
12. Russell J. The importance of pH in the regulation of ruminal acetate to propionate ratio and methane production in vitro. Journal of Dairy Science 1998, 81:3222-3230.
13. Calsamiglia S, Cardozo P, Ferret A, Bach A. Changes in rumen microbial fermentation are due to a combined effect of type of diet and pH. Journal of animal science 2008, 86:702-711.
14. Tveit A, Urich T, Svenning MM. Metatranscriptomic analysis of arctic peat soil microbiota. Applied and environmental microbiology 2014:AEM. 01030-01014.

15. NRC. Nutrient requirements of dairy cattle. 7th ed. National Research Council; 2001.
16. Ørskov E, McDonald I. The estimation of protein degradability in the rumen from incubation measurements weighted according to rate of passage. The Journal of Agricultural Science 1979, 92:499-503.
17. R development Core Team. R: A language and environment for statistical computing. http://wwwR-projectorg 2015.
18. Mertens D. Kinetics of cell wall digestion and passage in ruminants. Forage cell wall structure and digestibility 1993:535-570.
19. NFTA. National forage testing association reference method: dry matter by oven drying for 3 hours at 105 C. NFTA Reference Methods. National Forage Testing Association, Omaha, NB. 2006.
20. Van Soest Pv, Robertson J, Lewis B. Methods for dietary fiber, neutral detergent fiber, and nonstarch polysaccharides in relation to animal nutrition. Journal of dairy science 1991, 74:3583-3597.
21. AOAC. Official Methods of Analysis, 16th edition. Association of Official Analytical Chemists, Gaithersburg, MD 1997.
22. Kristensen NB. Quantification of whole blood short-chain fatty acids by gas chromatographic determination of plasma 2-chloroethyl derivatives and correction for dilution space in erythrocytes. Acta Agriculturae Scandinavica, Section A-Animal Science 2000, 50:231-236.
23. Bolger AM, Lohse M, Usadel B. Trimmomatic: a flexible trimmer for Illumina sequence data. Bioinformatics 2014, 30:2114-2120.
24. Kopylova E, Noé L, Touzet H. SortMeRNA: fast and accurate filtering of ribosomal RNAs in metatranscriptomic data. Bioinformatics 2012, 28:3211-3217.
25. Quast C, Pruesse E, Yilmaz P, Gerken J, Schweer T, Yarza P, Peplies J, Glöckner FO. The SILVA ribosomal RNA gene database project: improved data processing and web-based tools. Nucleic acids research 2012, 41:D590-D596.
26. Burge SW, Daub J, Eberhardt R, Tate J, Barquist L, Nawrocki EP, Eddy SR, Gardner PP, Bateman A. Rfam 11.0: 10 years of RNA families. Nucleic acids research 2012, 41:D226-D232.
27. Li F, Henderson G, Sun X, Cox F, Janssen PH, Guan LL. Taxonomic assessment of rumen microbiota using total RNA and targeted amplicon sequencing approaches. Frontiers in microbiology 2016, 7:987.
28. Zimin AV, Delcher AL, Florea L, Kelley DR, Schatz MC, Puiu D, Hanrahan F, Pertea G, Van Tassell CP, Sonstegard TS. A whole-genome assembly of the domestic cow, Bos taurus. Genome biology 2009, 10:R42.
29. Elsik CG, Tellam RL, Worley KC. The genome sequence of taurine cattle: a window to ruminant biology and evolution. Science 2009, 324:522-528.
30. Kim D, Pertea G, Trapnell C, Pimentel H, Kelley R, Salzberg SL. TopHat2: accurate alignment of transcriptomes in the presence of insertions, deletions and gene fusions. Genome biology 2013, 14:R36.

31. Callahan BJ, McMurdie PJ, Rosen MJ, Han AW, Johnson AJA, Holmes SP. DADA2: high-resolution sample inference from Illumina amplicon data. Nature methods 2016, 13:581.
32. Wang Q, Garrity GM, Tiedje JM, Cole JR. Naive Bayesian classifier for rapid assignment of rRNA sequences into the new bacterial taxonomy. Applied and environmental microbiology 2007, 73:5261-5267.
33. McMurdie PJ, Holmes S. phyloseq: an R package for reproducible interactive analysis and graphics of microbiome census data. PloS one 2013, 8:e61217.
34. Zerbino DR, Birney E. Velvet: algorithms for de novo short read assembly using de Bruijn graphs. Genome research 2008, 18:821-829.
35. Lombard V, Golaconda Ramulu H, Drula E, Coutinho PM, Henrissat B. The carbohydrate-active enzymes database (CAZy) in 2013. Nucleic acids research 2013, 42:D490-D495.
36. Henrissat B. A classification of glycosyl hydrolases based on amino acid sequence similarities. Biochemical Journal 1991, 280:309-316.
37. Henrissat B, Bairoch A. New families in the classification of glycosyl hydrolases based on amino acid sequence similarities. Biochemical journal 1993, 293:781-788.
38. Henrissat B, Bairoch A. Updating the sequence-based classification of glycosyl hydrolases. Biochemical Journal 1996, 316:695.
39. Davies G, Henrissat B. Structures and mechanisms of glycosyl hydrolases. Structure 1995, 3:853-859.
40. Henrissat B, Davies G. Structural and sequence-based classification of glycoside hydrolases. Current opinion in structural biology 1997, 7:637-644.
41. Coutinho PM, Deleury E, Davies GJ, Henrissat B. An evolving hierarchical family classification for glycosyltransferases. Journal of molecular biology 2003, 328:307-317.
42. Campbell JA, Davies GJ, Bulone V, Henrissat B. A classification of nucleotide-diphospho-sugar glycosyltransferases based on amino acid sequence similarities. Biochemical Journal 1997, 326:929.
43. Boraston AB, Bolam DN, Gilbert HJ, Davies GJ. Carbohydrate-binding modules: fine-tuning polysaccharide recognition. Biochemical Journal 2004, 382:769-781.
44. Lombard V, Bernard T, Rancurel C, Brumer H, Coutinho PM, Henrissat B. A hierarchical classification of polysaccharide lyases for glycogenomics. Biochemical Journal 2010, 432:437-444.
45. Edgar RC. Search and clustering orders of magnitude faster than BLAST. Bioinformatics 2010, 26:2460-2461.
46. Franzosa EA, McIver LJ, Rahnavard G, Thompson LR, Schirmer M, Weingart G, Lipson KS, Knight R, Caporaso JG, Segata N, et al. Species-level functional profiling of metagenomes and metatranscriptomes. Nat Methods 2018, 15:962-968.
47. Pinheiro J, Bates D, DebRoy S, Sarkar D, Team RC. nlme: Linear and nonlinear mixed effects models. R package version version 31-137 2018.

48. Bates D, Mächler M, Bolker B, Walker S. Fitting linear mixed-effects models using lme4. arXiv preprint arXiv:14065823 2014.
49. Gloor GB, Macklaim JM, Pawlowsky-Glahn V, Egozcue JJ. Microbiome datasets are compositional: and this is not optional. Frontiers in microbiology 2017, 8:2224.
50. Fernandes AD, Reid JN, Macklaim JM, McMurrough TA, Edgell DR, Gloor GB. Unifying the analysis of high-throughput sequencing datasets: characterizing RNA-seq, 16S rRNA gene sequencing and selective growth experiments by compositional data analysis. Microbiome 2014, 2:15.
51. Gloor GB, Reid G. Compositional analysis: a valid approach to analyze microbiome high-throughput sequencing data. Canadian journal of microbiology 2016, 62:692-703.
52. Aitchison J. The statistical analysis of compositional data. Journal of the Royal Statistical Society Series B (Methodological) 1982:139-177.
53. Li H. Microbiome, metagenomics, and high-dimensional compositional data analysis. Annual Review of Statistics and Its Application 2015, 2:73-94.
54. Lovell D, Pawlowsky-Glahn V, Egozcue JJ, Marguerat S, Bähler J. Proportionality: a valid alternative to correlation for relative data. PLoS computational biology 2015, 11:e1004075.
55. Hawinkel S, Mattiello F, Bijnens L, Thas O. A broken promise: microbiome differential abundance methods do not control the false discovery rate. Briefings in bioinformatics 2017.
56. Palarea-Albaladejo J, Martín-Fernández JA. zCompositions—R package for multivariate imputation of left-censored data under a compositional approach. Chemometrics and Intelligent Laboratory Systems 2015, 143:85-96.
57. Kassambara A, Mundt F. Factoextra: extract and visualize the results of multivariate data analyses. R package version 2016, 1:2016.
58. Harrell Jr FE, Dupont C. Hmisc: Harrell miscellaneous. R package version 4.0-3. Online publication 2017.
59. Wei T, Simko V. R package “corrplot”: Visualization of a Correlation Matrix (Version 0.84). URL https://github com/taiyun/corrplot 2017.
60. Li F, Guan LL. Metatranscriptomic profiling reveals linkages between the active rumen microbiome and feed efficiency in beef cattle. Applied and environmental microbiology 2017:AEM. 00061-00017.
61. Petri RM, Schwaiger T, Penner GB, Beauchemin KA, Forster RJ, McKinnon JJ, McAllister TA. Characterization of the core rumen microbiome in cattle during transition from forage to concentrate as well as during and after an acidotic challenge. PloS one 2013, 8:e83424.
62. Jami E, Mizrahi I. Composition and similarity of bovine rumen microbiota across individual animals. PloS one 2012, 7:e33306.
63. Henderson G, Cox F, Ganesh S, Jonker A, Young W, Collaborators GRC, Abecia L, Angarita E, Aravena P, Arenas GN. Rumen microbial community composition varies with diet and host, but a core microbiome is found across a wide geographical range. Scientific reports 2015, 5:14567.

64. De Mulder T, Goossens K, Peiren N, Vandaele L, Haegeman A, De Tender C, Ruttink T, de Wiele TV, De Campeneere S. Exploring the methanogen and bacterial communities of rumen environments: solid adherent, fluid and epimural. FEMS Microbiology Ecology 2017, 93.
65. Kang S, Evans P, Morrison M, McSweeney C. Identification of metabolically active proteobacterial and archaeal communities in the rumen by DNA-and RNA-derived 16 S rRNA gene. Journal of applied microbiology 2013, 115:644-653.
66. Li F, Hitch TC, Chen Y, Creevey CJ. Comparative metagenomic and metatranscriptomic analyses reveal the breed effect on the rumen microbiome and its associations with feed efficiency in beef cattle. Microbiome 2019, 7:6.
67. Leng R. The rumen–a fermentation vat or a series of organized structured microbial consortia: implications for the mitigation of enteric methane production by feed additives. Livestock Research for Rural Development 2011, 23:Article# 258.
68. Huo W, Zhu W, Mao S. Impact of subacute ruminal acidosis on the diversity of liquid and solid-associated bacteria in the rumen of goats. World Journal of Microbiology and Biotechnology 2014, 30:669-680.
69. Deusch S, Camarinha-Silva A, Conrad J, Beifuss U, Rodehutscord M, Seifert J. A structural and functional elucidation of the rumen microbiome influenced by various diets and microenvironments. Frontiers in microbiology 2017, 8:1605.
70. Gregorini P, Beukes P, Waghorn G, Pacheco D, Hanigan M. Development of an improved representation of rumen digesta outflow in a mechanistic and dynamic model of a dairy cow, Molly. Ecol Modell 2015, 313:293-306.
71. Legay-Carmier F, Bauchart D. Distribution of bacteria in the rumen contents of dairy cows given a diet supplemented with soya-bean oil. British Journal of Nutrition 1989, 61:725-740.
72. Myer PR, Smith TP, Wells JE, Kuehn LA, Freetly HC. Rumen microbiome from steers differing in feed efficiency. PloS one 2015, 10:e0129174.
73. Wang Z, Elekwachi CO, Jiao J, Wang M, Tang S, Zhou C, Tan Z, Forster RJ. Investigation and manipulation of metabolically active methanogen community composition during rumen development in black goats. Scientific reports 2017, 7:422.
74. Henderson G, Cox F, Kittelmann S, Miri VH, Zethof M, Noel SJ, Waghorn GC, Janssen PH. Effect of DNA extraction methods and sampling techniques on the apparent structure of cow and sheep rumen microbial communities. PLoS One 2013, 8:e74787.
75. Borrel G, Harris HM, Tottey W, Mihajlovski A, Parisot N, Peyretaillade E, Peyret P, Gribaldo S, O'Toole PW, Brugère J-F. Genome sequence of “Candidatus Methanomethylophilus alvus” Mx1201, a methanogenic archaeon from the human gut belonging to a seventh order of methanogens. Am Soc Microbiol; 2012.
76. Joblin K, Naylor G, Williams A. Effect of Methanobrevibacter smithii on xylanolytic activity of anaerobic ruminal fungi. Applied and Environmental Microbiology 1990, 56:2287-2295.

77. Franzolin R, Wright A-DG. Microorganisms in the rumen and reticulum of buffalo (Bubalus bubalis) fed two different feeding systems. BMC research notes 2016, 9:243.
78. Abrar A, Watanabe H, Kitamura T, Kondo M, Ban-Tokuda T, Matsui H. Diversity and fluctuation in ciliate protozoan population in the rumen of cattle. Animal Science Journal 2016, 87:1188-1192.
79. Akkada AA, Howard B. The biochemistry of rumen protozoa. 3. The carbohydrate metabolism of Entodinium. Biochemical Journal 1960, 76:445.
80. De Menezes AB, Lewis E, O'Donovan M, O'Neill BF, Clipson N, Doyle EM. Microbiome analysis of dairy cows fed pasture or total mixed ration diets. FEMS microbiology ecology 2011, 78:256-265.
81. Schulze A, Storm AC, Weisbjerg MR, Nørgaard P. Effects of forage neutral detergent fibre and time after feeding on medial and ventral rumen pH and volatile fatty acids concentration in heifers fed highly digestible grass/clover silages. Animal Production Science 2017, 57:129-132.
82. Plaizier JC, Li S, Danscher AM, Derakshani H, Andersen PH, Khafipour E. Changes in microbiota in rumen digesta and feces due to a grain-based subacute ruminal acidosis (SARA) challenge. Microbial ecology 2017, 74:485-495.
83. Franzolin R, Dehority B. Effect of prolonged high-concentrate feeding on ruminal protozoa concentrations. Journal of Animal Science 1996, 74:2803-2809.
84. Hook SE, Steele MA, Northwood KS, Wright A-DG, McBride BW. Impact of high-concentrate feeding and low ruminal pH on methanogens and protozoa in the rumen of dairy cows. Microbial ecology 2011, 62:94-105.
85. Wang L, Hatem A, Catalyurek UV, Morrison M, Yu Z. Metagenomic insights into the carbohydrate-active enzymes carried by the microorganisms adhering to solid digesta in the rumen of cows. PloS one 2013, 8:e78507.
86. Güllert S, Fischer MA, Turaev D, Noebauer B, Ilmberger N, Wemheuer B, Alawi M, Rattei T, Daniel R, Schmitz RA. Deep metagenome and metatranscriptome analyses of microbial communities affiliated with an industrial biogas fermenter, a cow rumen, and elephant feces reveal major differences in carbohydrate hydrolysis strategies. Biotechnology for biofuels 2016, 9:121.
87. Lynd LR, Zhang Y. Quantitative determination of cellulase concentration as distinct from cell concentration in studies of microbial cellulose utilization: analytical framework and methodological approach. Biotechnology and bioengineering 2002, 77:467-475.
88. Shallom D, Shoham Y. Microbial hemicellulases. Current opinion in microbiology 2003, 6:219-228.
89. Comtet-Marre S, Parisot N, Lepercq P, Chaucheyras-Durand F, Mosoni P, Peyretaillade E, Bayat AR, Shingfield KJ, Peyret P, Forano E. Metatranscriptomics reveals the active bacterial and eukaryotic fibrolytic communities in the rumen of dairy cow fed a mixed diet. Frontiers in Microbiology 2017, 8:67.
90. Nolan J, Leng R, Dobos R, Boston R. The production of acetate, propionate and butyrate in the rumen of sheep: fitting models to 14C-or 13C-labelled tracer data to determine synthesis rates and interconversions. Animal Production Science 2014, 54:2082-2088.

91. Sutton J, Dhanoa M, Morant S, France J, Napper D, Schuller E. Rates of production of acetate, propionate, and butyrate in the rumen of lactating dairy cows given normal and low-roughage diets. J Dairy Sci 2003, 86:3620-3633.
92. Schlau N, Guan L, Oba M. The relationship between rumen acidosis resistance and expression of genes involved in regulation of intracellular pH and butyrate metabolism of ruminal epithelial cells in steers. Journal of Dairy Science 2012, 95:5866-5875.
93. Sung HG, Kobayashi Y, Chang J, Ha A, Hwang IH, Ha J. Low ruminal pH reduces dietary fiber digestion via reduced microbial attachment. Asian Australasian Journal of Animal Sciences 2007, 20:200.
94. Stewart CS. Factors affecting the cellulolytic activity of rumen contents. Appl Environ Microbiol 1977, 33:497-502.
95. Hu Z-H, Yu H-Q, Zhu R-F. Influence of particle size and pH on anaerobic degradation of cellulose by ruminal microbes. International Biodeterioration & Biodegradation 2005, 55:233-238.

Table

Table 1. Functional pathways that were significantly different among treatments[1].

Pathway	Control		LpH		SEM	*P*value		
	Liquid	Solid	Liquid	Solid		Con vs LpH[2]	Con vs LpH[3]	Liquid vs Solid[4]
GLYCOLYSIS: glycolysis I (from glucose 6-phosphate)	0.25	0.33	0.09	0.28	0.07	0.05	0.53	0.03
PWY-5484: glycolysis II (from fructose 6-phosphate)	0.23	0.28	0.08	0.22	0.07	0.04	0.43	0.06
ILEUSYN-PWY: L-isoleucine biosynthesis I (from threonine)	0.12	0.27	0.07	0.24	0.05	0.50	0.60	0.002
PWY-5100: pyruvate fermentation to acetate and lactate	0.20	0.25	0.06	0.23	0.06	0.04	0.72	0.03
P108-PWY: pyruvate fermentation to propanoate	0.67	0.56	0.25	0.49	0.12	0.03	0.69	0.60

[1]Relative abundances of functional pathways were transformed to centered log ratio to avoid compositional data problem.
[2]Control versus LpH within the ruminal liquid fraction
[3]Control versus LpH within the ruminal solid fraction
[4]Ruminal sample fraction effect regardless of ruminal pH

Figures

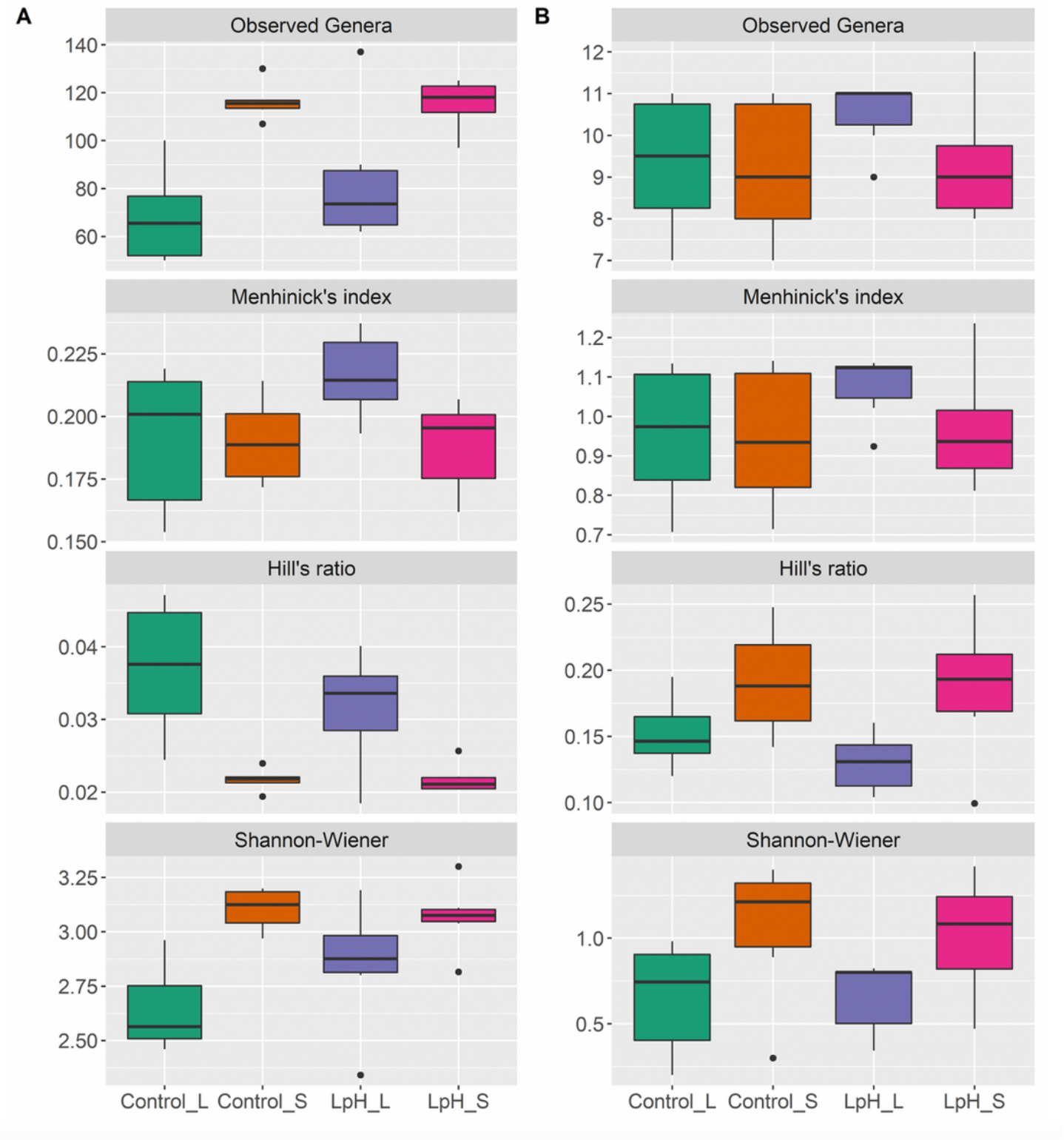

Figure 1

Effects of sampling phases and ruminal pH on observed genera, index of richness, evenness, and alpha diversity among treatments for bacterial (A) and protozoal (B) genera. Control_L and Control_S represent ruminal liquid and solid fraction at the Control group, and LpH_L and LpH_S represent ruminal liquid and solid fraction in the acid infusion group with a pH reduction of 0.5 units.

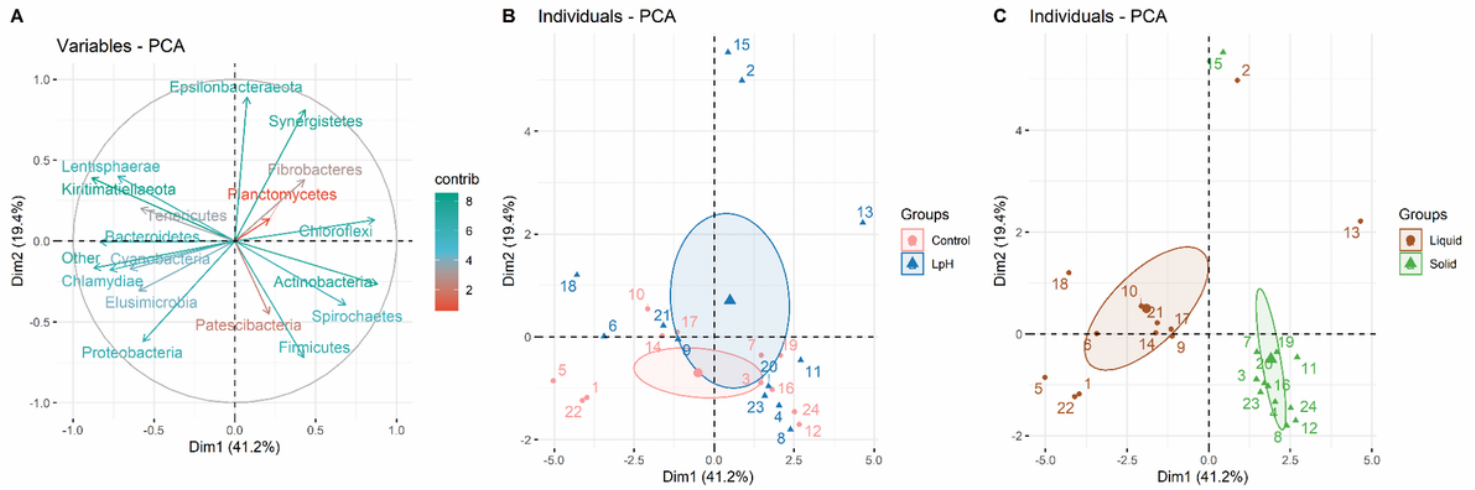

Figure 2

Principal component analyses (PCA) of overall bacterial composition among all samples at the phylum level. Variable contributions to the first two components are labelled with different colors (A). All variables were represented by arrows, and individuals were represented by points with numbers. Points were colored by treatment group (B) or ruminal sample fraction group (C). All the sequence counts were transformed to centered log ratios before PCA analyses.

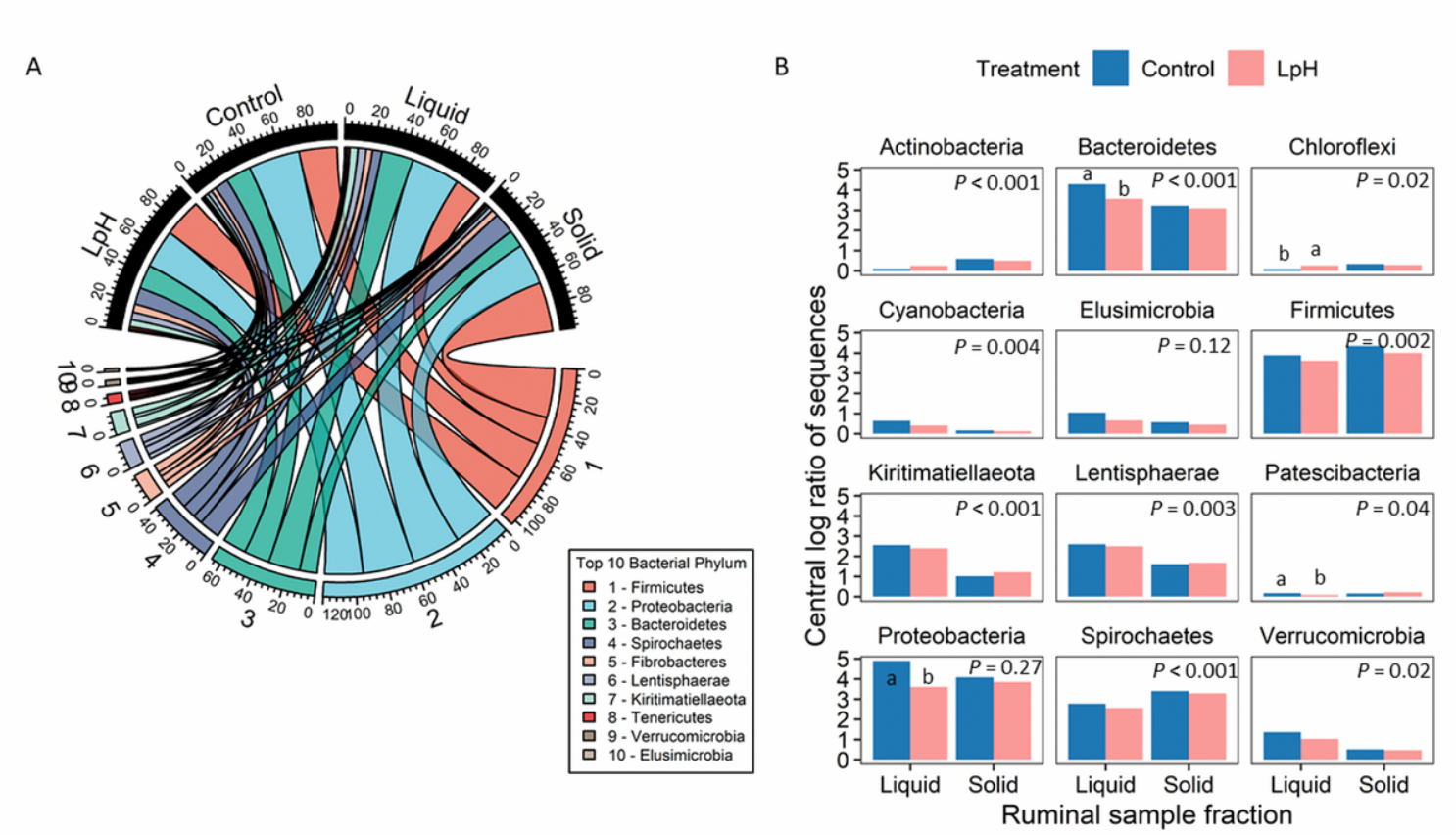

Figure 3

Taxonomic composition of the ruminal microbiome in the liquid and solid fractions in response to normal and low pH treatments. The top 10 bacterial phyla were selected, and sequences were expressed as relative abundance (A). The bar chart shows bacterial phyla that were significantly affected by treatment or by sample fraction (B). P value in each block shows difference between the liquid and sloid fraction, and different characters indicate significantly different means within the liquid or solid fraction. Results are reported as central log ratios of sequences where a value of 1 represents the mean ratio.

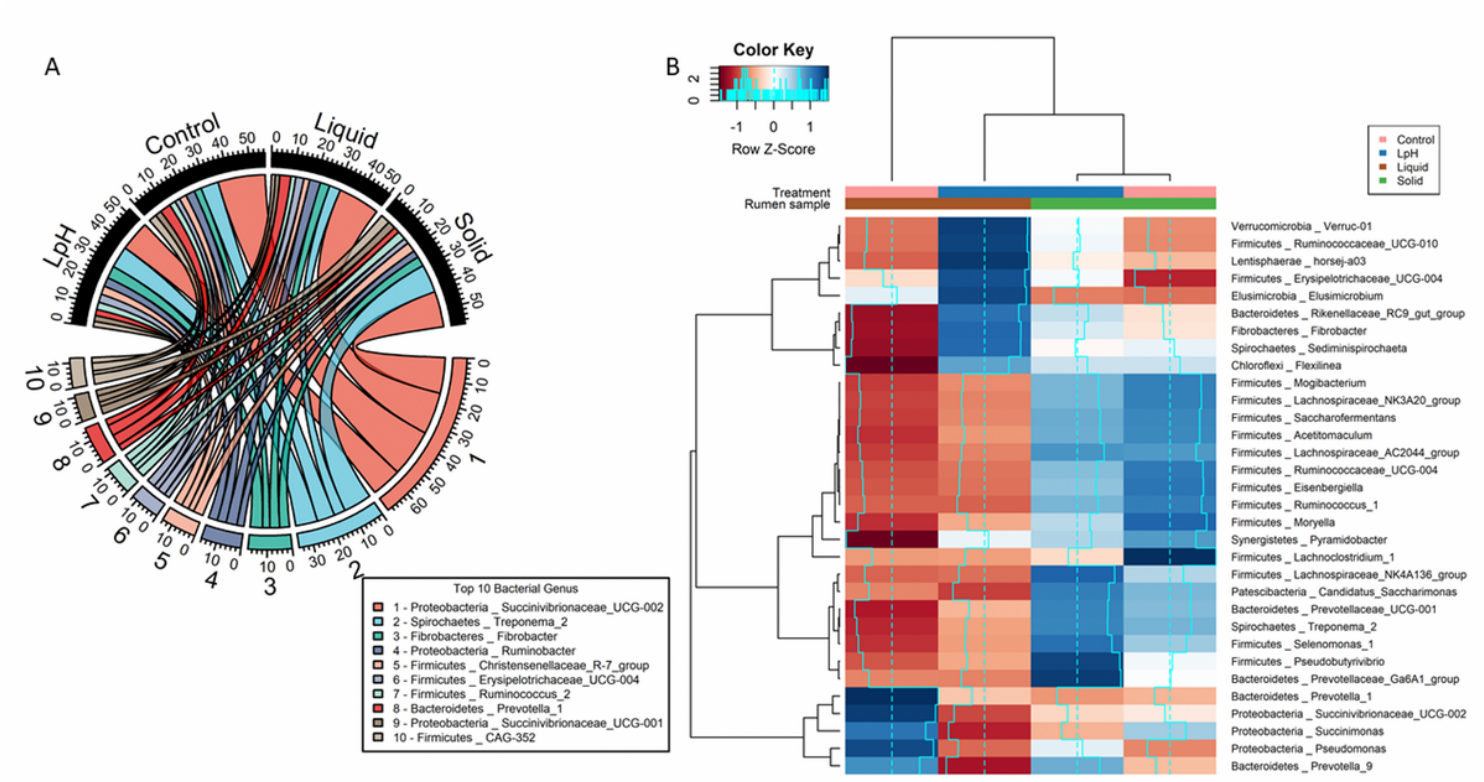

Figure 4

Taxonomic composition of the ruminal microbiome in the liquid and solid fractions in response to normal and low pH treatments. The top 10 bacterial genus were selected, and sequences were expressed as relative abundance (A). The heatmap shows bacterial genera that were significantly affected by pH and by sample fraction (B). Rows are color coded according to Z-score. A Z-score change of +1 is equal to one standard deviation above the row mean. Blue represents upregulation, and red represents downregulation.

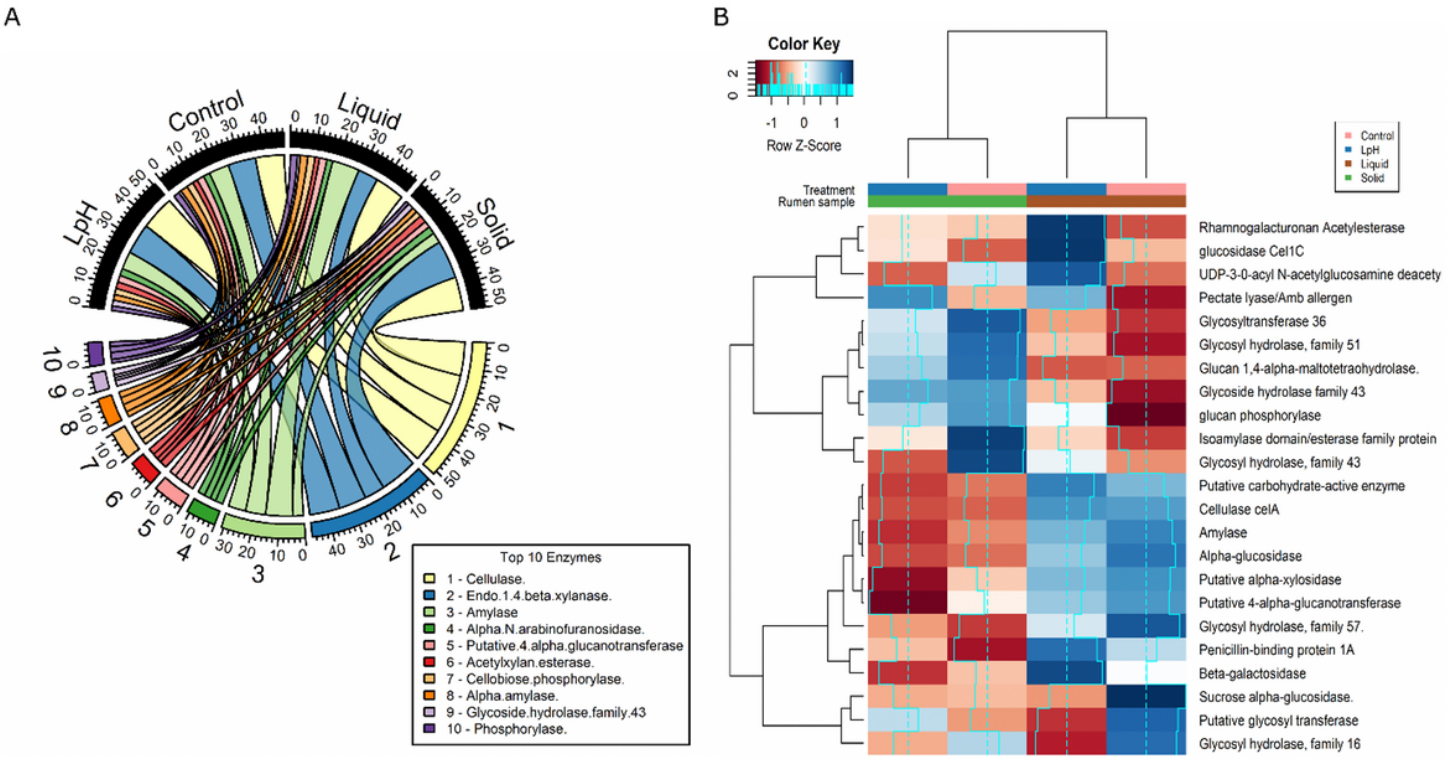

Figure 5

mRNA expressions of the carbohydrate-active degrading enzymes. The top 10 enzymes were selected (A). Sequence counts were expressed as relative abundance (%). Heatmap shows enzymes that were significantly affected by pH effect and sample fractions (B). Rows are color coded according to Z-score. A Z-score change of +1 is equal to one standard deviation above the row mean. Blue represents upregulation, and red represents downregulation.

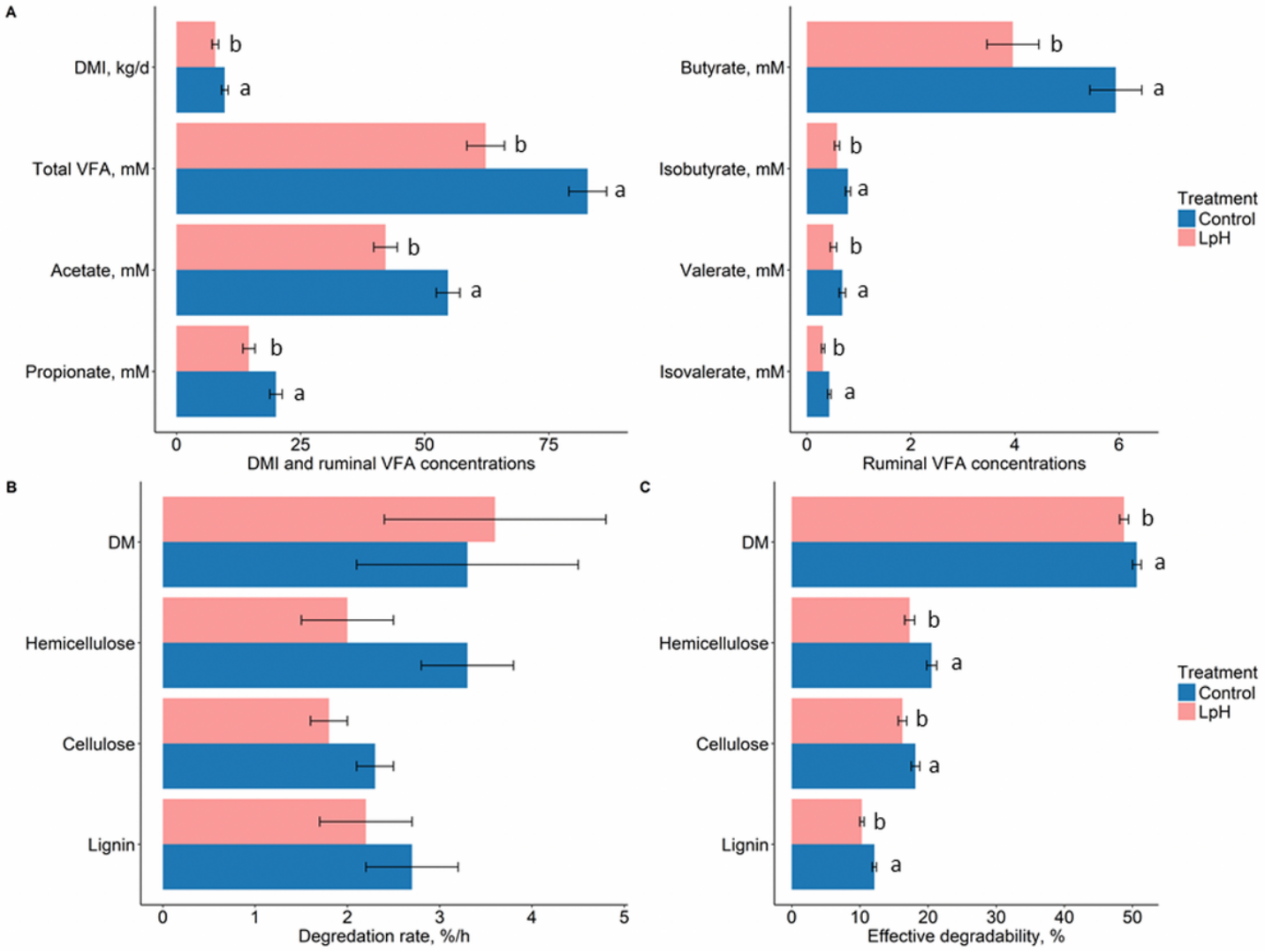

Figure 6

Effects of ruminal pH on DMI, fiber degradation, and ruminal volatile fatty acid concentrations. Different characters indicate significantly different means between normal and low pH treatment.

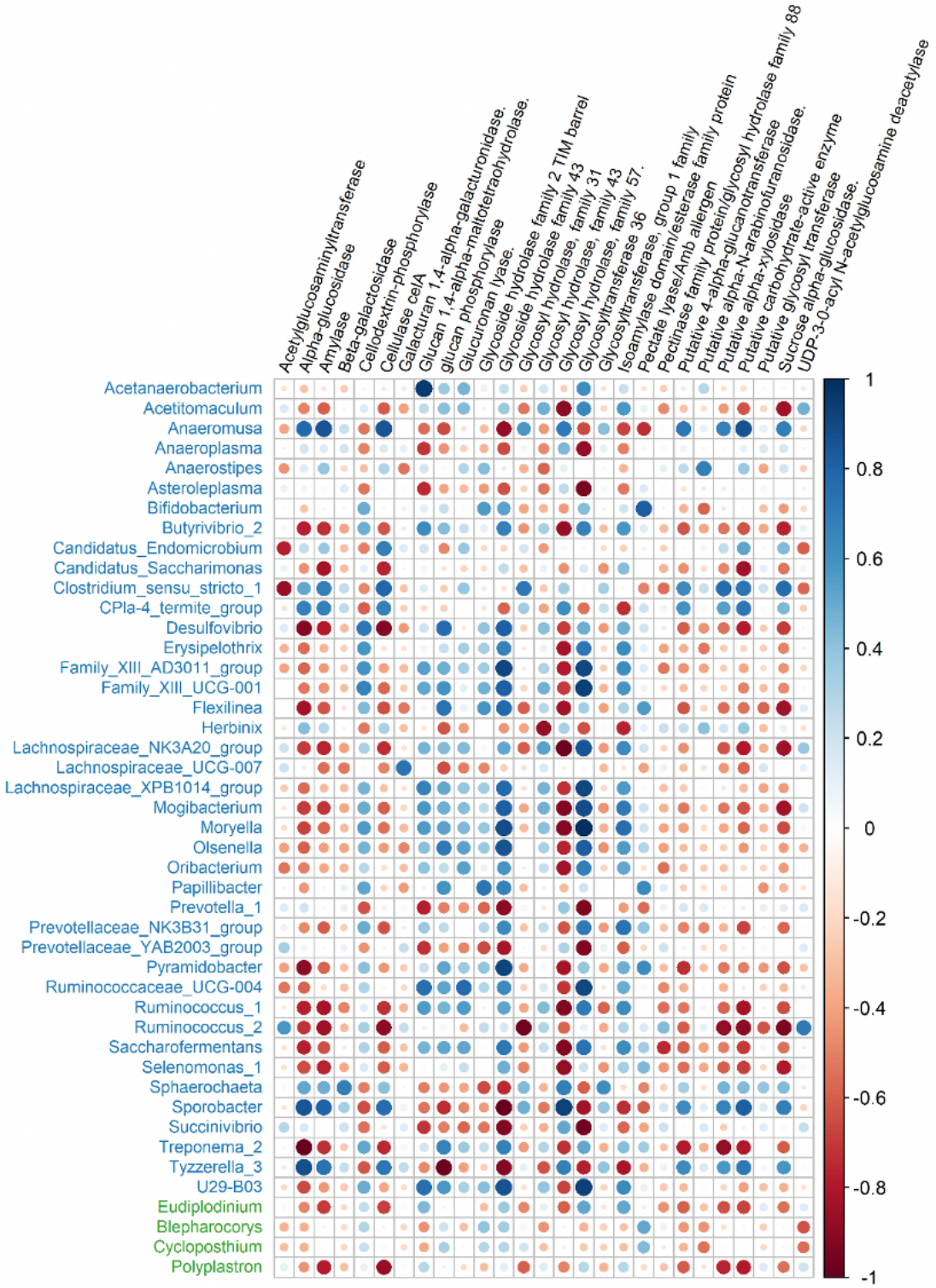

Figure 7

Pairwise correlations between microbial genera and carbohydrate-active degrading enzymes. Only the enzyme expressions that were significantly correlated with bacterial genera were shown (P value < 0.05, |r| > 0.5). The bacterial genera were colored by blue, and protozoan genera were colored by green.

Supplementary Files

This is a list of supplementary files associated with this preprint. Click to download.

- Lietal.2020RuminalpHSupplementR1.docx